MEMS Accelerometer Simulations in Matlab/SIMULINK and COMSOL Multiphysics

Jacek Nazdrowicz

***Abstract*—In this paper modelling and simulation of MEMS accelerometers in Matlab/SIMULINK environment are presented. Results of simulations of three different approaches: mathematical, electrical equivalent and physical models are compared with FEM accelerometer model created in COMSOL software. Results of simulations are analyzed for displacement response for two of the most popular spring geometries – folded and straight. Author takes into consideration crucial aspects of damping coefficients influence on accelerometer performance.**

***Index Terms*—Microelectromechanical systems, simulation model, microaccelerometer, MATLAB, SIMULINK, MEMS modeling, simscape toolbox.**

I. Principle of Operation of MEMS Accelerometer

MEMS accelerometer is a MEMS sensor for physical acceleration measuring. Acceleration can be caused by inertial forces or mechanical excitation. There are some different types of sensing but two stands out - piezoelectric and capacitive [2-3]. However electrostatic physics is most often willingly used because of easy of fabrication and good performance parameters.

MEMS capacitive accelerometer device consists of inertial mass suspended on springs anchored to substrate (fig. 1). This mass has also movable electrodes located on both sides. Whole is a mass-spring-damper system [5-6] [7]. On both sides of an accelerometer there are static electrodes anchored to substrate. Mass motion under external acceleration with voltage load presence allows to measure capacitance changes between static and movable electrodes which can be converted to other physical quantities [8].

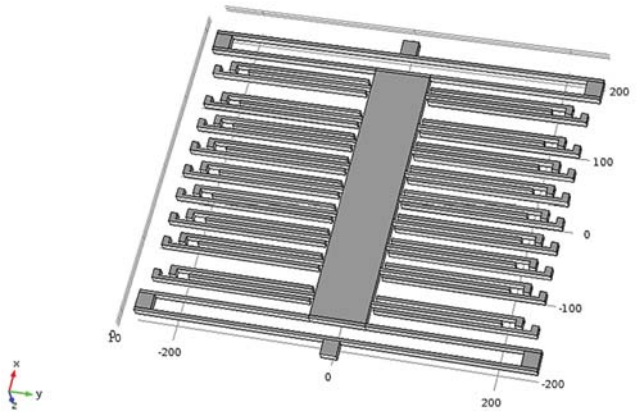

Fig. 1. Structure of MEMS accelerometer considered in this article.

J. Nazdrowicz is with the Department of Microelectronics and Computer Science, Lodz University of Technology, Lodz, Poland (email: jnazdrowicz@dmcs.pl)

Because such accelerometer has some moving parts – structure designs are focused on shape of springs, number of them and way of combination with inertial mass. Additionally they must be hanged properly to assure degradation, assure stability and obtain the best performance results. This obviously depends on spring shapes and anchor location. There are two main types of springs applied in motion sensors. First type is straight beam based - beams are mostly anchored at four points. The other type is folded beam based, which has small spring constant [9].

II. Theory Background of Accelerometer

MEMS accelerometers are modeled using a second order mass spring damper equation (1):

$$\begin{aligned} &F_x = F_a + F_b + F_k - F_{el} \Leftrightarrow \\ &\Leftrightarrow ma_x = m\frac{d^2x}{dt^2} + b\frac{dx}{dt} + kx - F_{el} \end{aligned} \tag{1}$$

where F_x – is external force acting on accelerometer, F_a - inertial force, F_b - damping force, F_k - elastic force, F_e – electrostatic force, k - spring constant, b - damping coefficient, m – proof mass.

Damping phenomena related to motion air molecules between electrodes is reflected in equation (1) as a damping coefficient:

$$b(x) = \frac{\mu A^2}{2}\left[\frac{1}{(x_0 - x)^3} + \frac{1}{(x_0 + x)^3}\right] \tag{2}$$

where $A=Lt$, L – length of capacitance electrodes, t - thickness..

Electrostatic force in equation (1) comes from the fact that device is loaded with voltage ($V_1=Vsin(\omega t)$, $V_2=-Vsin(\omega t)$). The comb structure of proof mass and anchored electrodes causes appearance two opposite directed forces F_1 and F_2 and based on them:

$$F_{el} = F_1 - F_2 = \frac{\varepsilon_0 A}{4}\left(\frac{V_1^2}{(x_0 - x)^2} - \frac{V_1^2}{(x_0 + x)^2}\right) \tag{3}$$

Finally, the equation (1) including (2), (3) and (4) has a following form:

$$m\frac{d^2x_x}{dt^2} = m\frac{d^2x}{dt^2} + \left(\frac{\mu A^2}{2}\left[\frac{1}{(x_0-x)^3} + \frac{1}{(x_0+x)^3}\right]\right)\frac{dx}{dt} + \\ + kx - \left(\frac{\varepsilon_0 A V^2 \sin^2(\omega t)}{2}\left[\frac{1}{(x_0-x)^2} - \frac{1}{(x_0+x)^2}\right]\right) \quad (4)$$

where x_0 is the initial distance between fixed and moving plate (in equilibrium state), μ – air viscosity, A – area of the sense electrode formed by comb-drive electrodes.

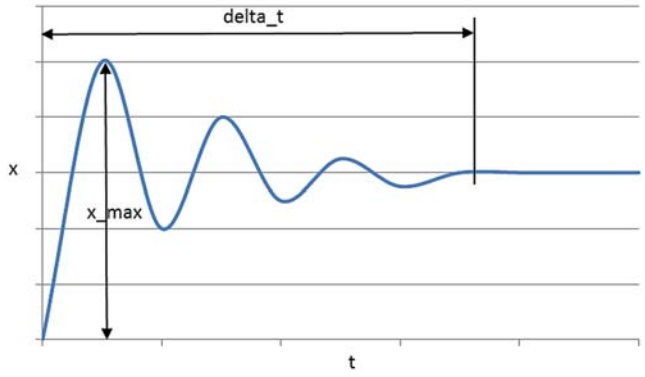

Fig. 2. Characteristic of proof mass displacement in MEMS accelerometer.

The equation (4) returns x which is fundamental for later capacitances calculations. However before final displacement value establishes, inertial mass-spring system vibrates around that value. Because system is damped in first period it achieves the largest maximum (x_{max}) (fig. 2). This fact is extremely important in terms of geometrical dimensions of particular accelerometer parts and should be taken into consideration to avoid degradation of them. Another parameter which is important in point of view device application is time of displacement stabilization (Δt), which should be as short as possible - it influences on speed of sensor response. Considering the above the geometry design is strongly oriented to optimize both stabilization time and displacement amplitude.

III. Modeling MEMS Accelerometer

Modeling and Simulation of MEMS accelerometer is complex task, because to obtain optimal performance parameters some physics domains need to be considered and additionally phenomenon nonlinearities, complex geometries, fluctuating external conditions. Therefore to optimize MEMS accelerometer performance parameters it is important to use Finite Element Method which is foundation of COMSOL software.

A. COMSOL multiphysics model

Model designed in COMSOL Multiphysics has folded beams-based springs located on both sides of inertial mass (fig. 1). It was created with many geometrical dimension variables, what allows user to parametrize it before meshing and running solver. To limit calculations model uses symmetry boundary conditions what can be seen in fig. 3.

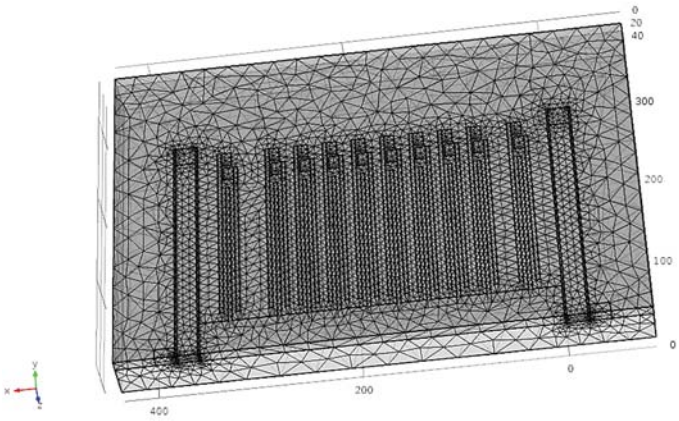

Fig. 3. Model of meshed MEMS accelerometer, with symmetry boundary condition implemented (view from bottom).

Because FEM simulation takes much time it can turn out that more simple models can be used. Of course, one of the method is to decrease finite element count, limit some geometry details like number of electrode fingers or apply symmetries, but time always will play main role here especially in transient simulations. Therefore FEM analysis can be supported or replaced with analysis in SIMULINK software.

In literature we can find some accelerometer models and simulations proposed and presented by authors [1,3,4]. Here three different approaches to model MEMS accelerometers in SIMULINK will be presented.

B. Mathematical model of MEMS device

In mathematical model equation (1) is implemented in SIMULINK using standard mathematical blocks. Model of accelerometer based on this approach is presented in fig. 4. This model consists of two integration blocks to obtain velocity and displacement from accelerometer. Geometry details can be inserted to calculate total mass of the system. Based on displacement values of particular capacitance components can be calculated for further signal processing. System was tested with constant acceleration value loaded. Material used in simulations was Polysilicon.

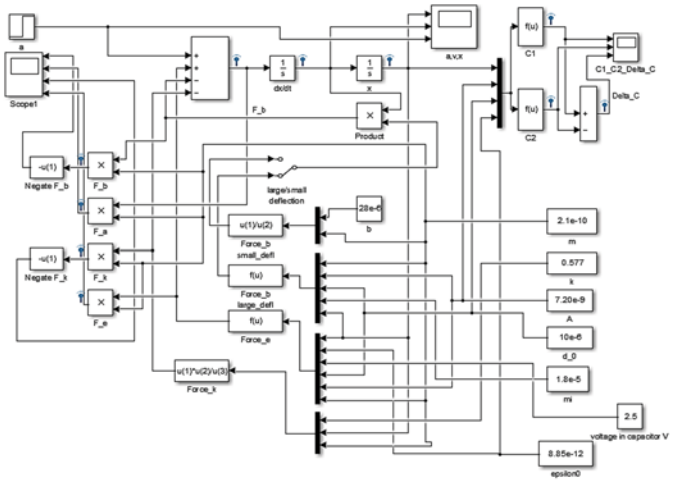

Fig. 4. Matlab/SIMULINK mathematical model of MEMS accelerometer.

C. Electrical equivalent model of MEMS device

Second model was created with use of analogies of mechanical and electrical quantities which are presented in Table I. Particular forces in mechanical domain can be transformed to electrical domain (mass can be replaced with capacitance, spring constant with inverse of inductance and damping coefficient with inverse of resistance). External force causes acceleration can be simulated with controlled current source.

TABLE I.
LIST OF ELECTRICAL ANALOGIES FOR MODEL.

Mechanical Quantity	Electrical Quantity
v - velocity	*V* - voltage
F – force	*I* - current
m – mass	*C* - capacitance
b – damping	*1/R*, R - resistance
k – spring coefficient	*1/L* - inductance

Referring to (1) and Table I we can see that velocity can be replaced with voltage, displacement and acceleration is obtained by velocity integration and derivative respectively. Transformed equation is following:

$$I = C\frac{dV}{dt} + \frac{1}{R}V + \frac{1}{L}\int V dt$$

In fig. 5 there is electrical equivalent model of MEMS gyroscope presented. In brief, this is vibrating circuit RLC.

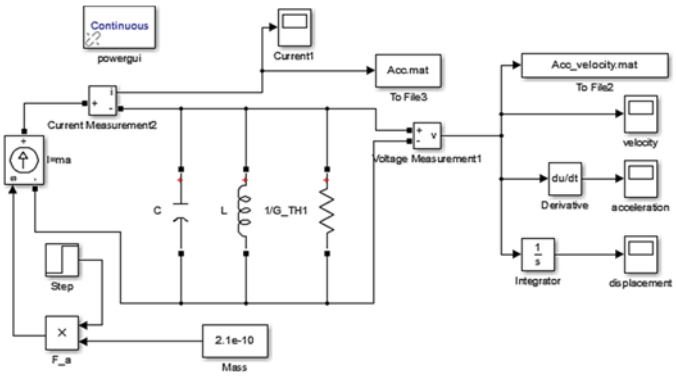

Fig. 5. Matlab/SIMULINK electrical equivalent model of MEMS Accelerometer.

D. Physical model of MEMS accelerometer

To model MEMS accelerometer Simscape™ toolbox was also used. It allows to connect particular parts of system as they exist in real world. However these particular parts do not reflect geometrical shapes. Simscape toolbox also includes accelerometer integrated block to simplify meaningfully model. In fig. 6 there is such accelerometer model presented, created with linear motion blocks.

For given models mass was calculated in SIMULINK with use particular component masses and compared to mass value obtained from COMSOL software. Spring coefficient was calculated by using following formulas:

$$k_b = \frac{E \cdot w \cdot t^3}{4 \cdot L^3}, k_p = \sum_i k_{bi}, \frac{1}{k_s} = \sum_i \frac{1}{k_{bi}}, k_{tot} = \frac{k_b}{2} \quad (5)$$

where: k_b – spring coefficient for single beam, E – Young's Modulus, t – thickness, L – length, w – width of beam.

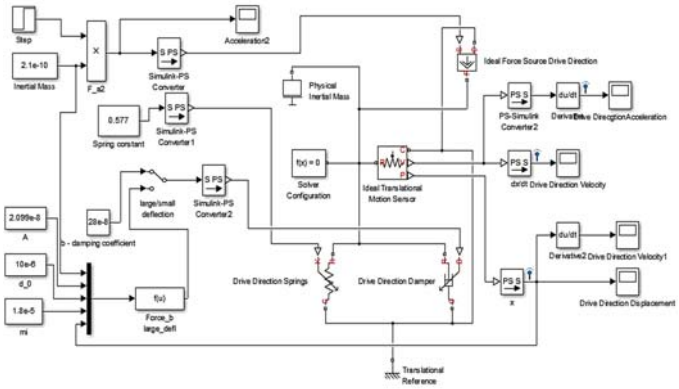

Fig. 6. Matlab/SIMULINK physical model of MEMS accelerometer.

IV. SIMULATION RESULTS

In Table II there are geometrical and material parameters presented which were used in modeling and simulation.

TABLE II.
LIST OF GEOMETRICAL AND MATERIAL PARAMETERS.

Symbol	Displacement	Value
m	Calculated proof mass	$2.1*10^{-9}$kg
μ	Air viscosity	$1.8 \cdot 10^{-5}$Ns/m^2
k	Calculated spring coefficient	0.577N/m
V	Voltage load	2.5V
ε_o	Permitivity coefficient	$8.854*10^{12}$ F/m,
A	Electrode area	$7.20*10^{-9}$m^2
ρ	Density (Polysilicon)	2328 kg/m^3

At the beginning simulation of models implemented in SIMULINK were compared to this one created in COMSOL environment. Example results are presented in fig. 7. Simulation time was 0.001s. For FEM model verification purposes system was loaded with constant 2*g* acceleration. Result of displacement in stationary simulation reaches maximum at $7.64*10^{-9}$m. The same results are obtained in transient simulation for all three presented models. Because stable displacement value is quickly achieved, capacitances behave similarly.

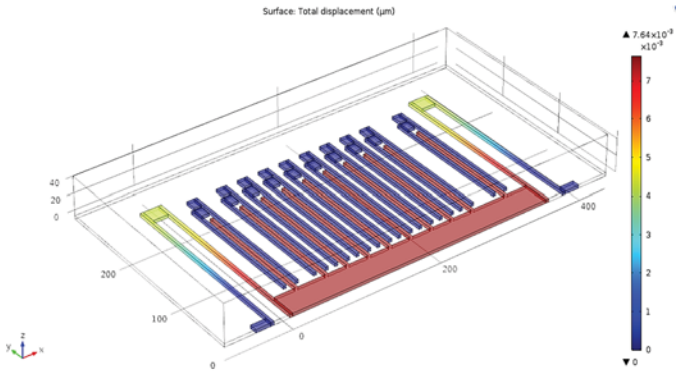

Fig. 7. Displacement results under simulation in COMSOL using data from Table II.

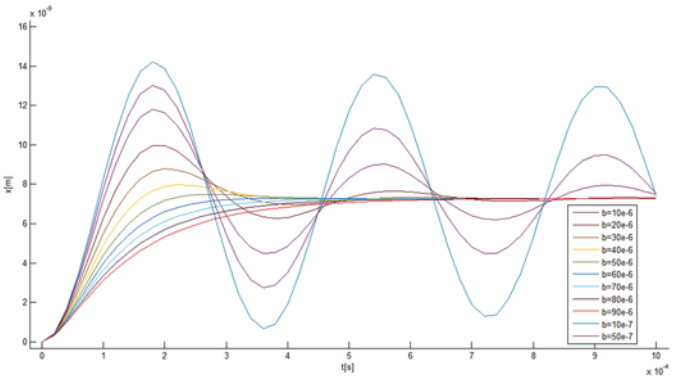

Fig. 8. Displacement results under simulation in SIMULINK using data from Table II with various damping coefficients. Calculated spring coefficient was k=0.544.

A. *Simulations with different damping coefficients*

In fig. 8, 9, 10 there are results of simulation presented for accelerometer with various damping coefficients from range between $10*10^{-7}$ and $90*10^{-6}$ and spring constant k=0.544. We may observe that there is threshold value of damping coefficient which changes definitely accelerometer behavior for given other accelerometer parameters like geometrical dimensions or material properties. Here the value of damping coefficients equals to $50*10^{-6}$. Decrease this value causes system to vibrate before it stabilizes. Although when this value is in range $30*10^{-6}$ - $50*10^{-6}$ vibrations are very small – after first period system reaches final displacement value and amplitude of displacement is very small. For damping coefficient lower than $30*10^{-6}$ number of vibrations grows before system stabilizes of its displacement. Moreover, time of this stabilization process grows and takes much longer than window time taken in these simulations. Additionally, along with damping coefficient decrease maximum amplitude of displacement grows meaningfully and for b=$10*10^{-7}$ final (stabilized) value is almost two times higher ($14*10^{-9}$m).

When damping coefficient is higher than threshold value (>$50*10^{-6}$) system does not vibrate. Since damping is very strong, system smoothly reaches final displacement value.

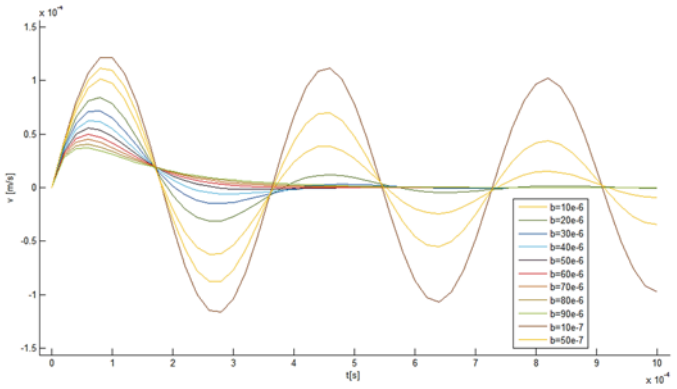

Fig. 9. Velocity results under simulation in SIMULINK using data from Table II with various damping coefficients. Calculated spring coefficient was k=0.544.

Very important is fact that stabilization time changes in time. We can conclude that increase of damping coefficient is effective (we do not have unnecessary vibrations which can degrade sensing comb). However – the optimal b value is $50*10^{-6}$, because it guarantees that this time is the shortest. Above and below this value – stabilization time increases; for lower damping coefficient – more meaningfully.

In fig. 9 plots for velocity in time are presented. We observe that velocity changes above and below zero value. System stops moving the fastest for threshold damping coefficient, too.

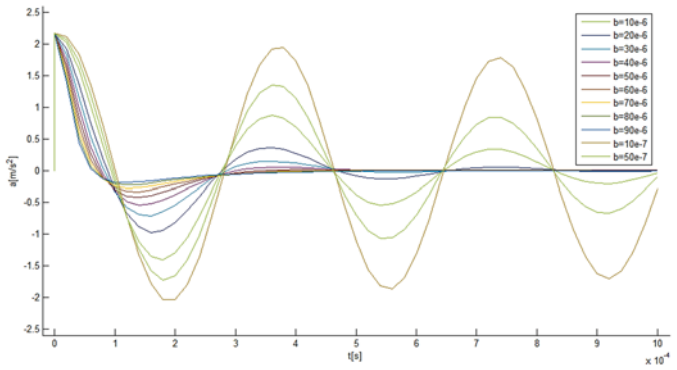

Fig. 10. Acceleration results under simulation in SIMULINK using data from Table II with various damping coefficients. Calculated spring coefficient was k=0.544.

Next plot (fig. 10) – acceleration dependency in time confirms what was described earlier – system has optimal response for threshold value and acceleration drops similarly (for first period of vibration) in whole scope of damping coefficient taken in simulations (compare slope of plots in first period).

Previous results were performed for constant acceleration value a=20m/s^2. In real world acceleration values and direction can change very fast. Accelerometer should also respond effectively and measure physical quantity. Next tests were performed for more complex entry signals.

In fig. 11 there is entry acceleration signal presented. At the beginning a=20m/s^2. Next it drops immediately to 5m/s^2 and then 0m/s^2. In fig. 12 displacement response is shown for this signal and for three different damping coefficients value (equal, lower and higher threshold value).

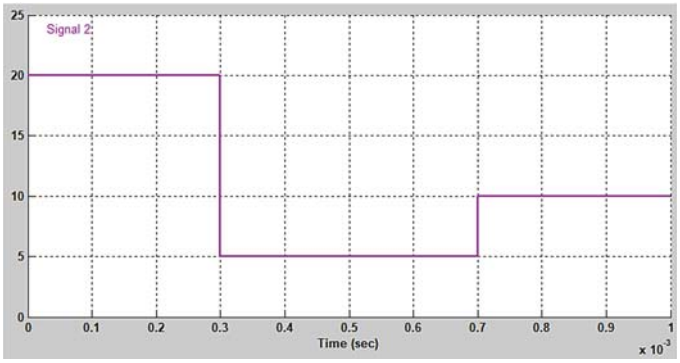

Fig. 11. Accelerations applied to accelerometer (same direction).

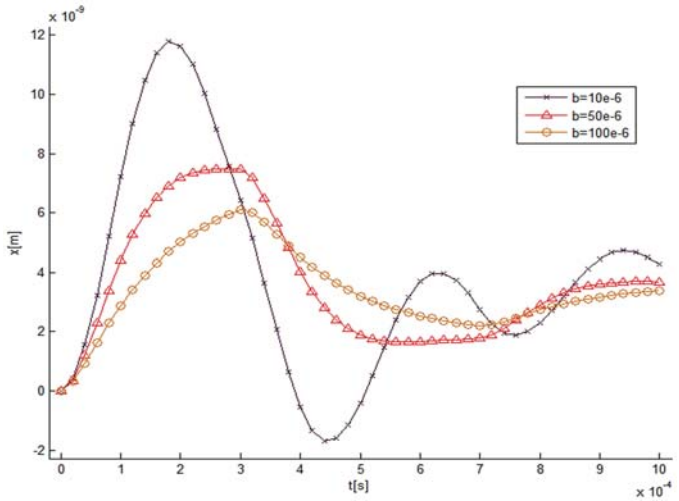

Fig. 12. Displacement results under simulation in SIMULINK using data from Table II with various damping coefficients and different applied acceleration (same direction). Calculated spring coefficient was k=0.544.

For b=10*10^{-6} we observe that inertial mass displacement changes meaningfully and no specified value of displacement is set. When applied acceleration changes, the fluctuation also changes – again there is no displacement stabilization. After acceleration stops – inertial mass still vibrates. Such system is useless.

For b=100*10^{-6} situation is better – large damping causes more predictable behavior of accelerometer, but relative long time of displacement stabilization causes, that it is not enough time (t=0.3*10^{-4}s) to measure accurately acceleration and in effect – there is a falsified result. System with such damping coefficient responses immediately and there is no unnecessary inertia motions. For b=50*10^{-6} (optimal value) system responses optimally, it reaches final value fast even after under acceleration changes. However notice that time of increase or decrease in this device takes 2*10^{-4}s. In case of faster acceleration changes – error results exponentially rise or drops depend on time.

Second case was for signal which reflects acceleration value changes and acceleration vector direction (fig. 13). As we can see in fig. 14 system behaves similarly. However for small damping coefficient (b=10*10^{-6}) we observe large amplitude in opposite direction (1.6*10^{-8}m) during fluctuation in compare to forward direction (1.3*10^{-8}m), even though absolute value of acceleration is the same. For larger damping coefficients displacement responses are much better.

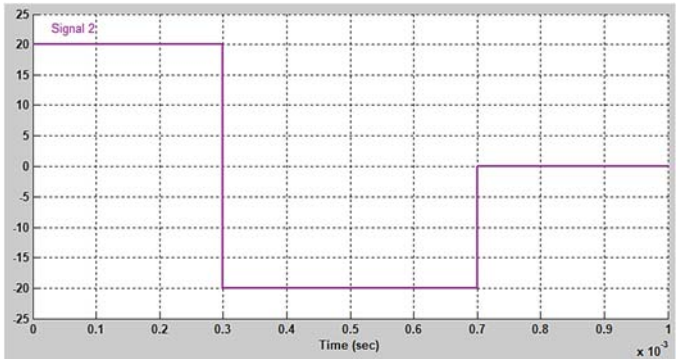

Fig. 13. Accelerations applied to accelerometer (opposite direction).

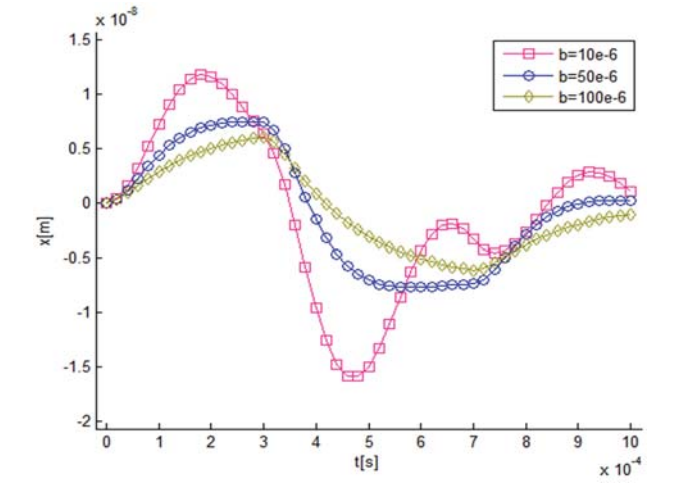

Fig. 14. Displacement results under simulation in SIMULINK using data from Table II with various damping coefficients and different applied acceleration (opposite direction). Calculated spring coefficient was k=0.544.

B. *Different spring length simulations*

Fig. 15 presents von Misses stress distribution and deformation of folded beams shapes. We can observe that edge parts of spring beams are exposed to the maximum stresses. These parts are mostly exposed to damage. This is enormously important in model with small damping coefficient (see previous results) – because there are many oscillations (often unpredictable) before inertial mass reaches its final value of displacement. Middle parts of beams are negligibly stressed even in case of meaningful deformation.

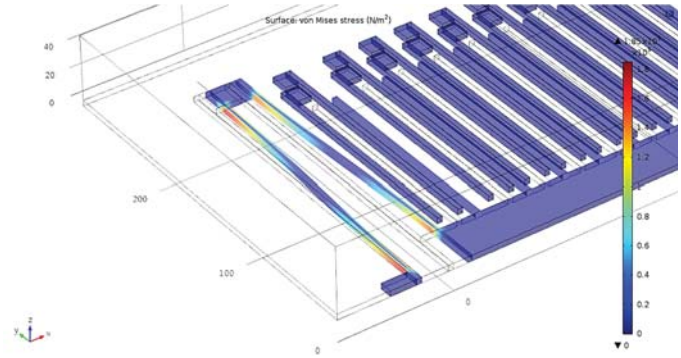

Fig. 15. Von Misses stresses distribution along folded spring beams.

Fig. 16 presents depedency of displacement in time for different length of single spring beam (obviously different spring constant). Results of simulations show that maximum displacement (during vibrations) is significantly large. This determines minimum distance between electrodes and distance between particular parts of spring beams.

In fig. 17 one can see that effective, maximum and minimum displacements which strongly depend on length of spring beam. For small changes of displacement detection it is good to have as large effective displacement as possible, but unfortunately maximum displacement is much larger. As a result, it limits significantly range of acceleration. Another negative consequence of such oscillations is faster fatigue of the material.

There is possible to change displacement response with geometrical dimension change. Fig. 18 shows results of such modifications (W_{spr} – width of beam spring, W_f- width of electrode finger). While slimming down finger electrode (and decreasing total moving mass – from $6.9739*10^{-10}$kg to $6.0830*10^{-10}$kg) displacement also decreases, what it is not good result. The only way to improve output is to slim down beam spring (in the simulation it was decreased 2 times – from $4*10^{-6}$m to $2*10^{-6}$m; mass decreased – from $6.9739*10^{-10}$kg to $6.1944*10^{-10}$kg). One can be observed in fig. 15 - displacement response increases twice and time decreases to $5*10^{-4}$s.

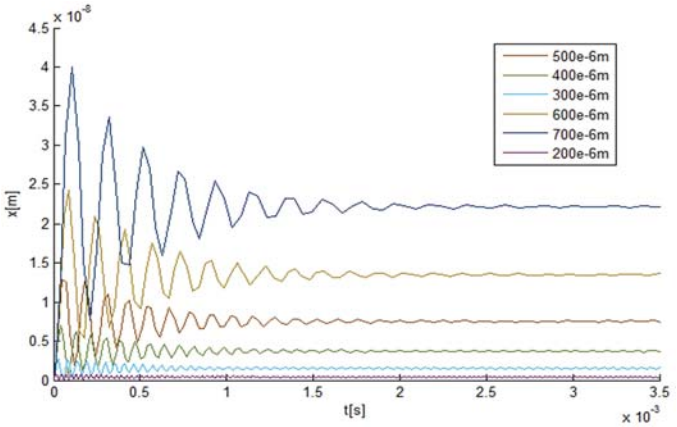

Fig. 16. Displacement results under simulation in SIMULINK for various spring beam length.

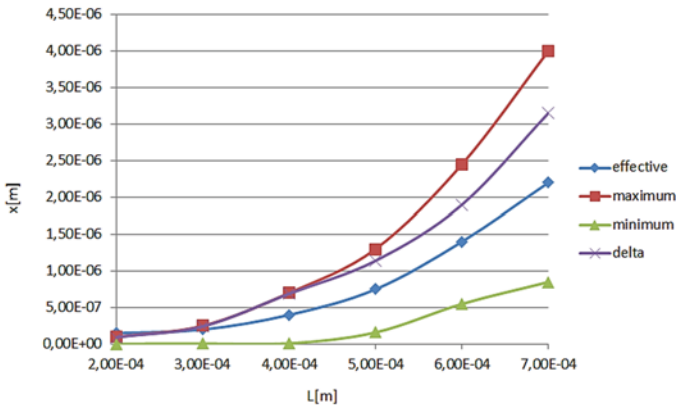

Fig. 17. Minimum, maximum, delta, effective displacement for various spring beam length.

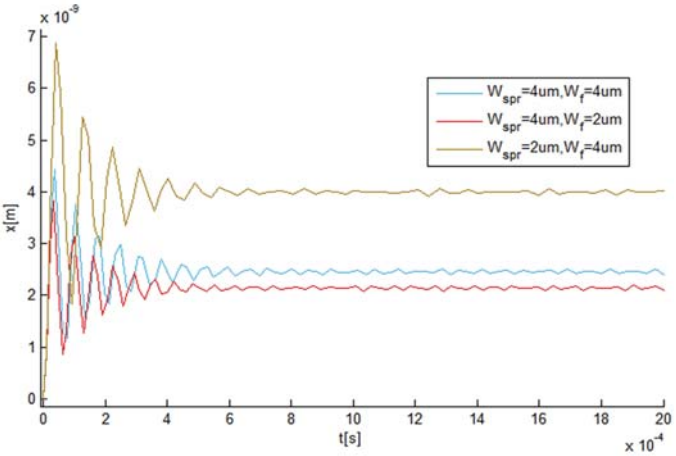

Fig. 18. Response characteristics in dependance of spring beam and finger electrode (thickness is constant = $12*10^{-6}$m), length spring $L=700*10^{-6}$m.

V. Conclusions

Damping coefficients and spring constants are physical quantities which decide about response characteristics motion sensors like MEMS accelerometers are typical mechanical system. Results show response time (what can evaluate measurement usability), are strongly connected with damping coefficient.. There is threshold value of damping coefficient which meaningfully changes accelerometer dynamical response. It turned out that this value is optimal for this device operation. Simulations presented here showed also that the meaningful impact on displacement amplitude, oscillations and time of displacement stabilization have spring shape and geometrical dimensions of electrodes.

Three types of MEMS accelerometer models were presented and results of simulation obtained were the same.

Because problem of geometry optimization is multidimensional and therefore very complex, only some important aspects were considered here and some of all important parameters were changed to expose areas to future research.

References

[1] Ming Hui Chang , Han Pang Huang. Simulation and characterization of a CMOS-MEMS gyroscope with parasitic insensitive sensing. ARSO pp. 1-6, 2008.

[2] N. Maluf, K. Williams, An Introduction to MicroElectromechanical Systems Engineering, 2th ed Artech House Inc., pp. 79-131, 2004.

[3]]Weiping Chen, Jinling Ding, Xiaowei Liu, Chao Wang, Design and system-level simulation of a capacitive dual axis accelerometer, Proceedings of the 2nd IEEE International Conference on Nano/Micro Engineered and Molecular Systems January 16 - 19 2007, Bangkok, Thailand.

[4] G. L. Teodor, The Matlab/Simulink modeling and numerical simulation of an analogue capacitive micro-accelerometer. Part 1: Closed loop MEMSTECH: pp. 115-121, 2008.

[5] A. Lawrence, Modern Inertial Technology: Navigation, Guidance and Control, .Springer Verlag, New York,1993.

[6] V. Kempe, Inertial MEMS: Principles and Practice, Cambridge University Press, pp. 227-282, 2011.

[7] G. Zhang, Sensing and Control Electronics for Low-Mass Low-Capacitance MEMS Accelerometer, *Ph.D. Dissertation*, Carnegie Mellon University, 2002, https://www.ece.cmu.edu/~mems/pubs/pdfs/ece/phd_thesis/0201_wu-2002.pdf.

[8] L. Zimmermann, J. Ebersohl, F. Le Hung, J. P. Berry, F. Baillieu, P. Rey, B. Diem, S. Renard, P. Caillat, Airbag application: a microsystem including a silicon capacitive accelerometer, CMOS switched capacitor electronics and true self-test capability. Sensors and Actuators, pp. 190-195, 1995.

[9] P. Singh, P. Srivastava, R. Kumari Chaudary, P. Gupta, Effect of Different proof mass supports on Accelerometer sensitivity, IEEE ICEETS, pp. 896-900, Apr. 2013.

Jacek Nazdrowicz was born in Poddębice, Poland, in 1975. He received the MSc degrees in Technical Physics (Computer Physics), Computer Sciences (Software Engineering and Networking Systems) and Marketing and Management from the Lodz University of Technology, Poland, in 1999, 2000 and 2001 respectively and the PhD degree in Economics Sciences, Management discipline, in Lodz University of Technology, in 2013.

From 2014 he attends doctoral study in Lodz University of Technology, electronics discipline. His research interests include modelling and simulation MEMS devices and their application in medicine. He participated in EduMEMS project (Developing Multidomain MEMS Models for Educational Purposes). He also educates in COMSOL software. Now he participates in Strategmed project (supported by the National Center for Research and Development)

Between 2007 and 2016 he worked in mBank as a System Engineer of SQL Server databases. He has the following certifications: MCSA Windows 2012, MS SQL Server 2012 and Storage Area Network (SAN) Specialist.

Since 2016 he also works in Fujitsu Technology Solutions in Lodz in Remote Infrastructure Management Department in Storage Team as a Storage Engineer (SAN Infastructure, Brocade, Netapp, Eternus products). He educates in many data storage and backup technologies (IBM, DELL/EMC, Hitachi, Fujitsu).